0026-895X/99/050883-11$3.00/0

MOLECULAR PHARMACOLOGY, **55:**883–893 (1999).

Single-Channel Kinetics of the Rat Olfactory Cyclic Nucleotide-Gated Channel Expressed in *Xenopus* Oocytes

JUN LI[1] and HENRY A. LESTER

Division of Biology, California Institute of Technology, Pasadena, California

Received September 24, 1998; accepted January 28, 1999

This paper is available online at http://www.molpharm.org

ABSTRACT

Cyclic nucleotide-gated channels are nonselective cation channels activated by intracellular cAMP and/or cGMP. It is not known how the binding of agonists opens the channel, or how the presumed four binding sites, one on each subunit, interact to generate cooperativity. We expressed the rat olfactory cyclic nucleotide-gated channel α subunit in *Xenopus* oocytes and recorded the single-channel currents. The channel had a single conductance state, and flickers at −60 mV showed the same power spectrum for cAMP and cGMP. At steady state, the distribution patterns of open and closed times were relatively simple, containing one or two exponential components. The conductance properties and the dwell-time distributions were adequately described by models that invoke only one or two binding events to open the channel, followed by an additional binding event that prolongs the openings and helps to explain apparent cooperativity. In a comparison between cAMP and cGMP, we find that cGMP has clearly higher binding affinity than cAMP, but only modestly higher probability of inducing the conformational transition that opens the channel.

Cyclic nucleotide-gated (CNG) channels play important roles in visual and olfactory signal transduction. They are activated by the direct binding of cAMP or cGMP to sites located at the intracellular side of channel protein (Fesenko et al., 1985; Zimmerman and Baylor, 1986; Nakamura and Gold, 1987). Because phosphorylation by cyclic nucleotide-dependent protein kinases is not involved, the activation and deactivation can take place at higher speed than in kinase-dependent pathways. The direct activation appears well suited for an important function in vertebrates: to mediate the detection of external stimuli by the peripheral sensory neurons of the visual and olfactory systems. In this regard the CNG channels resemble ion channels that are gated by extracellular ligands, such as the nicotinic acetylcholine receptors, which mediate fast communication between cells.

Molecular cloning data have revealed that CNG channels form a family of related proteins (reviewed in Yau, 1994; Finn et al., 1996). For each cloned channel subunit, the deduced amino acid sequence contains a "core" channel domain, followed by a carboxyl terminal cyclic nucleotide-binding domain. Similar to voltage-gated channels, the "core" has six putative transmembrane segments and a P region, which comprise part of the pore. In other important aspects, however, the CNG channels differ from a typical voltage-gated channel. First, unlike the voltage-dependent Na^+ or K^+ channels, the CNG channels are poorly selective among monovalent cations. Second, their activities depend only slightly on membrane potential; apparently the conformational changes involved in activation are energetically coupled more tightly to ligand binding than to changes in membrane potential.

Despite these differences from voltage-gated channels, it is generally believed that each CNG channel, similar to a voltage-gated channel, is formed by the association of four subunits, each possessing its own cyclic nucleotide-binding site. Thus the activation of CNG channels may involve, or even require, the binding of agonist molecules at all four binding sites. This would extend the similarity with voltage-gated channels, for which the conformational changes at all four "voltage sensors" contribute to the opening transition (see for example Hoshi et al., 1994; Stefani et al., 1994). The participation of multiple binding events during CNG channel activation is supported by the dose-response relations of the macroscopic currents: the Hill coefficient, an empirical measure of apparent cooperativity, is almost always greater than 1, and usually falls between 2 and 3 (Zimmerman and Baylor, 1986; Li et al., 1997).

An important goal of studies on CNG channels is to understand the mechanism of channel activation, especially how the binding events are coupled to the opening of the pore, and how the presumed four channel subunits interact to generate the apparent cooperativity. A companion paper reports struc-

This research was supported by a grant from the National Institutes of Health (NS-11756).

[1] Present address: Department of Genetics, Stanford University, 300 Pasteur Dr., M310, Stanford CA 94305

ABBREVIATIONS: CNG, cyclic nucleotide-gated; rOCNC1, rat olfactory channel, first subunit; rOCNC2, rat olfactory channel, second subunit.

ture-function studies on the CNG binding site (Li and Lester, 1999). To approach this goal it is also appropriate to examine the stochastic behavior of individual channels, because the macroscopic current, reflecting the collective activity of many channels, lacks the resolution to describe closely related models. It is also appropriate to examine the stochastic behavior of individual channels, because the macroscopic current, reflecting the collective activity of many channels, lacks the resolution to describe closely related models. In this regard, single-channel measurements provide a much richer set of data; in fact, they are among the few methods for monitoring the behavior of a single allosteric protein in real time. Furthermore, they allow us to recognize individual kinetic states and to specify the rate constants governing the transitions among them.

A number of laboratories have recorded single-channel currents of CNG channels. However, efforts toward a quantitative rather than merely descriptive kinetic analysis were previously hindered by at least three factors. 1) Channel openings are often flickery, i.e., the open-close transition are too brief for the recording apparatus to resolve (Matthews and Watanabe, 1988; Ildefonse et al., 1992; Sesti et al., 1994; Taylor and Baylor, 1995; Bucossi et al., 1997). 2) Many types of CNG channels open to multiple conductance levels (Taylor and Baylor, 1995; Liu et al., 1996; Bucossi et al., 1997; Ruiz and Karpen, 1997; Liu et al., 1998). When there is no clear correspondence between binding states and conductance classes, the multiplicity of conductance only complicates kinetic analysis. 3) Most studies used channels expressed in native tissues (Matthews and Watanabe, 1988; Sesti et al., 1994; Taylor and Baylor, 1995), in which the channel population is not homogeneous: the channel that is being recorded can be of any subunit composition out of the many different possibilities.

Here we report a study that circumvents some of these problems. We found that the α subunit of the rat olfactory CNG channel, rOCNC1, when expressed in *Xenopus* oocytes, displayed a single conductance and opened to a relatively stable current level. We therefore examined the kinetic characteristics of these single, homogeneous CNG channels under steady-state conditions. We found that 1) the openings showed no conspicuous clustering, in contrast both to predictions of some common models and to properties of many other ligand-gated channels; 2) with more ligands bound the open state was further stabilized, whereas the closed state was further destabilized, just as predicted by allosteric models; and 3) the open- and closed-time distributions displayed only a limited number of distinguishable components; as a result, simple kinetic models invoking one or two binding events and one or two gating transitions can account for the observed kinetic properties.

To estimate kinetic parameters, we used the maximum interval-likelihood method (Qin et al., 1996, 1997), in which the probability of observing an actual sequence of events, according to a given scheme, is simply the joint probability of observing these events individually and in the observed sequence. The algorithm searches for the parameters that maximize this probability. The final likelihood score of a model is used to compare it with alternative models. The comparison employs objective, statistical criteria for penalizing over-parameterization (Horn, 1987).

During the analysis, special attention was given to the comparison between cAMP and cGMP, both of which can activate rOCNC1. Previous studies show that cGMP has a ~20-fold lower EC_{50} than cAMP, although both produce the same maximal activation (Varnum et al., 1995; Gordon and Zagotta, 1995a,b). The present study verifies this finding and asks whether it arises 1) because of differences in the initial ligand-channel interaction, or 2) because of differences in the subsequent conformational transitions that open the channel (Li et al., 1997). The previous studies, based on macroscopic currents, assigned (2) as the likely explanation (Varnum et al., 1995; Gordon and Zagotta, 1995a,b). The single-channel kinetic study now suggests that explanation (1) holds: cGMP probably binds with much higher affinity, but the conformational changes are only modestly more likely than for cAMP.

Materials and Methods

Expression. All experiments were carried out on the rat olfactory CNG channel α subunit (Dhallan et al., 1990), kindly provided by Dr. K. W. Yau. The cDNA was subcloned (at *Eco*RI and *Hin*DIII) into the pGEMHE vector, originally constructed by E. R. Liman, containing the 5′ and 3′ untranslated sequences of the *Xenopus laevis* major β-globin gene for enhanced expression in oocytes (Liman et al., 1992). Stage V and VI *Xenopus laevis* oocytes were injected with cRNA synthesized in vitro (Ambion T7 mMESSAGE mMACHINE Kit, Ambion Inc., Austin, TX) from plasmid linearized with *Pst*I. To obtain patches that contain only one channel, we injected oocytes with 50 nl of each of three serial dilutions of cRNA, covering a concentration range of ~16-fold. The highest concentration of the three dilutions varied from 1 to 50 μg/ml, depending on the month-to-month variations in expression levels, and to allow recordings to be performed from 24 to 120 h after injection. To improve the viability of oocytes, horse serum (HyClone Laboratories, Logan, UT) was added at 5% to the incubation solution ND96 (Quick et al., 1992). ND96 contains: 96 mM NaCl, 2 mM KCl, 1 mM $MgCl_2$, 1.8 mM $CaCl_2$, and 5 mM HEPES (pH 7.4).

All recordings were performed from inside-out patches at room temperature exposed to symmetrical solutions containing: 140 mM NaCl, 5 mM HEPES, and 0.2 mM EDTA (pH 7.4). The oocytes were stripped as described (Quick and Lester, 1994), and membrane seals were formed in ND96 with the pipette potential held at −60 mV. The patch was then excised by withdrawing the pipette, at which moment we observed the endogenous current flowing through the Ca^{2+}-activated Cl^- channels. The perfusion solutions containing various concentrations of cAMP or cGMP were locally applied to the patch using an RSC100 rapid solution changer (Molecular Kinetics, Pullman, WA). Upon perfusion of the divalent cation-free solution with no cyclic nucleotide, the endogenous Ca^{2+}-activated Cl^- current disappeared, leaving a patch with a typical resistance of 4 to 15 GΩ. cAMP and cGMP were both obtained from Sigma Chemical Co. (St. Louis, MO).

Recording and Signal Processing. The recording pipettes were fabricated from filamented, borosilicate glass tubing (Corning type 7740, *A*. 1.5 mm, i.d. 0.86 mm, Sutter Instrument Co. Novato, CA), using a Flaming/Brown Micropipette Puller (model P-87, Sutter Instrument Co.). The pipette tips were fire-polished (MF-83, Narishige Scientific Instrument Lab, Tokyo, Japan). The filled pipettes had resistances between 5 and 15 MΩ in the bath solution.

Macroscopic and single-channel currents were recorded with an Axopatch 200A patch clamp amplifier (Axon Instruments, Foster City, CA) with a CV201A headstage, which has a feedback capacitor of 1 picofarad (pf). For single-channel recordings, the four-pole low-pass Bessel filter on the Axopatch 200A was opened at its widest at 50 kHz (f_{-3dB}). The data were sampled at 44 kHz by a NeuroCorder Digitizing Unit (Model DR384, NeuroData Instruments Corp., New York), and subsequently stored on videotape. The NeuroCorder em-

ploys a predigitizing, anti-aliasing filter with a rolloff of 70 dB within 1.5 kHz of 22 kHz (−3 dB frequency).

During analysis, data were played back and converted to analog form by the NeuroCorder. Unless otherwise stated, data were filtered at 2 kHz with an eight-pole lowpass Bessel filter (model 902, Frequency Devices Inc., Haverhill, MA), and digitized at 10 kHz with FETCHEX of pCLAMP 6, via a Digidata 1200 interface (Axon Instruments).

We analyzed recordings from patches containing a single channel. This was verified by the lack of double openings during prolonged periods of activity with high open probabilities such as when $P_{open} > 80\%$.

Power spectra of cAMP- and cGMP-activated single channel currents were computed using a fast Fourier transform procedure in Origin 5.0 (Microcal Software, Northampton, MA). The currents were filtered at 10 kHz (corner frequency) with an eight-pole lowpass Bessel filter and digitized at 50 kHz. Transformation was carried out on data segments of 16384 sampling points covering a continuous open or closed period, and used a Hamming window. Power spectra of cyclic nucleotide-induced currents are the difference between spectra in the presence of cyclic nucleotides and in its absence. We fitted the spectra with a single Lorentzian function:

$$P(f) = \{P_0 / [1+(f / f_c)^2]\} + P_1,$$

where P(f) is the power at frequency f, P_0 is the 0 Hz power plateau, P_1 is the frequency-independent component (white noise), and f_c is the corner frequency of the Lorentzian function.

Kinetic Modeling. The data were idealized in FETCHAN of pCLAMP 6 using a half-magnitude threshold-crossing criterion for detecting event transitions. Transitions were individually inspected and manually accepted or rejected. The resulting event-list files were converted into ASCII form, and were selected for further analysis by 1) discarding files that were apparently nonstationary, judged by inspecting the opening probability, the open times, or the closed times, and 2) discarding files with fewer than 800 events. For the selected files, open- and closed-time histograms were constructed in PSTAT of pCLAMP 6, and were fitted in PSTAT with sums of exponential functions using the Levenberg-Marquardt method with weighting by function. The histograms were binned with a logarithmic time axis and plotted with a square-root transformation of the vertical axis, so that the individual exponential components could be directly visualized as apparent peaks in the histograms (Sigworth and Sine, 1987). We verified that openings as brief as 90 μs could be detected at 50% of the original signal amplitude by passing pulses through the NeuroCorder-filter-computer combination. This value was used 1) to transform the event lists by deleting durations shorter than 90 μs and joining the adjacent events (Colquhoun and Sigworth, 1995), and 2) as the lower limit of the fitting range while we fit the histograms with exponential functions. In this study we used the time constant and relative fraction of the exponential functions for describing the main characteristics of data, whereas the kinetic rate constants were estimated using the maximum interval-likelihood method (see below).

We converted each event-list file in ASCII format into a dwell-time file format (.dwt) readable by the maximum-interval-likelihood program (MIL). MIL is used for estimating, with a correction for missed events, the kinetic parameters from idealized single-channel records (Qin et al., 1996, 1997). The Windows 95 version of MIL was kindly provided by Drs. Feng Qin, Anthony Auerbach, and Fred Sachs (Department of Biophysical Sciences, State University of New York at Buffalo). Ninety microseconds was used as the "dead time" in MIL for missed-event correction.

Results

In this study we focused on the rOCNC1 homomeric channel. The rOCNC1/rOCNC2 heteromeric channels resemble the native channels more closely, but they are likely to coassemble with varied and undefined stoichiometry, each probably having a distinct set of functional characteristics. It has been known that presence of rOCNC2 raises the apparent sensitivity to cAMP (Bradley et al., 1994; Liman and Buck, 1994). Furthermore in the oocyte expression system, rOCNC2 causes desensitization, which is absent in the rOCNC1 homomeric channel (Liman and Buck, 1994). It is certainly true that the native olfactory channels are likely to be heteromeric. However, in this study, seeking a better understanding of the activation mechanism, we exploited the greater simplicity of homomeric channels.

We used the oocyte expression system. In the past, the HEK293 cell system has served well for our macroscopic studies. The expression level was high and was highly reproducible. HEK293 cells have the major drawback, however, that it is nearly impossible to isolate single channels: the channels tend to form clusters, even at the lowest levels of expression that we tested. The expression level in *Xenopus* oocytes, in contrast, seems to depend more linearly on the amount of mRNA injected, and the channels are distributed more evenly in the plasma membrane.

CAMP and cGMP Produce Similar Maximal Macroscopic Responses. The ligand selectivity of the olfactory CNG channels is very different from that of photoreceptor channels: although cGMP is a much more potent agonist than cAMP for the rod channels (Fesenko et al. 1985), both agonists can fully activate the olfactory channels (Nakamura and Gold, 1987; Zufall et al., 1994). It has been reported that the cloned rat olfactory channel rOCNC1 can be activated to roughly equal maximal levels by cAMP and cGMP (Dhallan et al., 1990; Gordon and Zagotta, 1995b). We confirmed this finding in our macroscopic recordings. For the patch shown in Fig. 1, cAMP activated 96% of the current activated by saturating cGMP. Two other patches yielded maximal current ratios between cAMP and cGMP of 99% and 87%, respec-

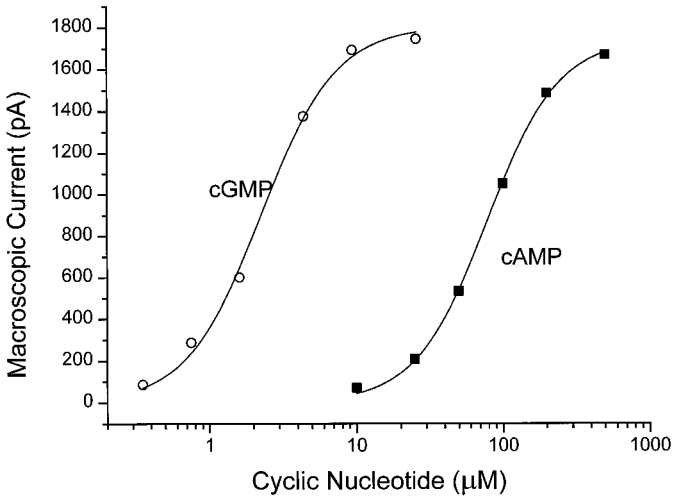

Fig. 1. Dose-response relation for macroscopic currents activated by cAMP and cGMP in a representative excised patch at $V_m = -80$ mV. The smooth lines are fits to Hill equation: $I = I_{max}/(1 + (EC_{50}/cNMP)^n)$, where I_{max} is maximal current, EC_{50} is concentration that activates 50% of maximal current, cNMP is concentration of cyclic nucleotides, and n is the Hill coefficient. I_{max}, EC_{50} and n were free parameters. For patch shown, I_{max} for cAMP is 96% of I_{max} for cGMP (1743 pA versus 1804 pA). Other parameters are: EC_{50} for cAMP, 78 μM; for cGMP, 2.7 μM; n for cAMP, 1.8; and for cGMP, 1.9.

tively. In contrast, for the bovine rod channels, cAMP activates less than 1% of the current activated by saturating concentrations of cGMP (see for example, Gordon and Zagotta, 1995b).

Basic Characteristics of Single Channels. Figure 2 presents consecutive current traces showing openings of a homomeric rOCNC1 channel, recorded at +60 mV and −60 mV, respectively, exposed to 50 μM cAMP at the cytoplasmic face. At +60 mV the channel opened to a single, relatively stable conductance level. The lack of subconductance and lack of flicker stand in clear contrast to the native rat olfactory CNG channels (Frings et al., 1992), the expressed homomeric bovine photoreceptor CNG channel (Ruiz and Karpen, 1997), and expressed heteromeric channels (Bradley et al., 1994; Liman and Buck, 1994; Liu et al., 1996, 1998). At −60 mV the open-channel noise became noticeably larger, indicating unresolved brief closings that interrupt opening. The baseline noise, however, was not increased at −60 mV, suggesting that there are few unresolved brief openings.

The brief closings could either be due to fast open-channel block, for instance by protons (Root and MacKinnon, 1994), or to fast conformational transitions intrinsic to the channel protein. The open-channel noise is characterized more completely in Fig. 7 below, and we conclude that cAMP and cGMP share similar kinetics for these brief closings. Opening up the lowpass filter would admit more noise, severely interfering with the visual inspection process during idealization. Therefore for most of the recordings we maintained filtering at 2 kHz.

Figures 3 shows consecutive current traces for a channel activated by 5 μM cGMP and 100 μM cAMP. The channel open probabilities were comparable in Fig. 3, A and B. Comparisons are pursued more thoroughly below, but it is evident that the conductance and broad kinetic features were similar between the two agonists.

Positive membrane potentials tend to destabilize the seal, and in most batches of oocytes, they activate endogenous stretch-activated channels within 20 s after the seal is formed. These channels are nonselective among monovalent cations, and we found that they are similar to rOCNC1 in many other aspects as well, including channel conductance and kinetic appearances. We therefore sought to avoid contamination of our records by these stretch-activated channels. For this reason most of the data reported here were recorded at −60 mV, a voltage at which the stretch-activated channels were no longer active.

We did, however, measure the conductance of a channel at various voltages between −10 mV and −150 mV (Figure 4). Throughout this range the conductance was linear and measured 45 pS. We have observed conductances varying from 35 to 46 pS in different recordings, with 80% of the measurements falling in the 40 to 45 pS range. The reason for this variability is not clear. For any given channel, however, the measured conductance was invariant during the course of the experiment. We did not observe any correlation between kinetic properties and the conductance of the channel.

The open probability (P_{open}) was measured from the idealized event lists using PSTAT. To illustrate the progression of channel activity, we individually calculated P_{open} for consecutive time segments of 2 or 4 s in length. Within each seg-

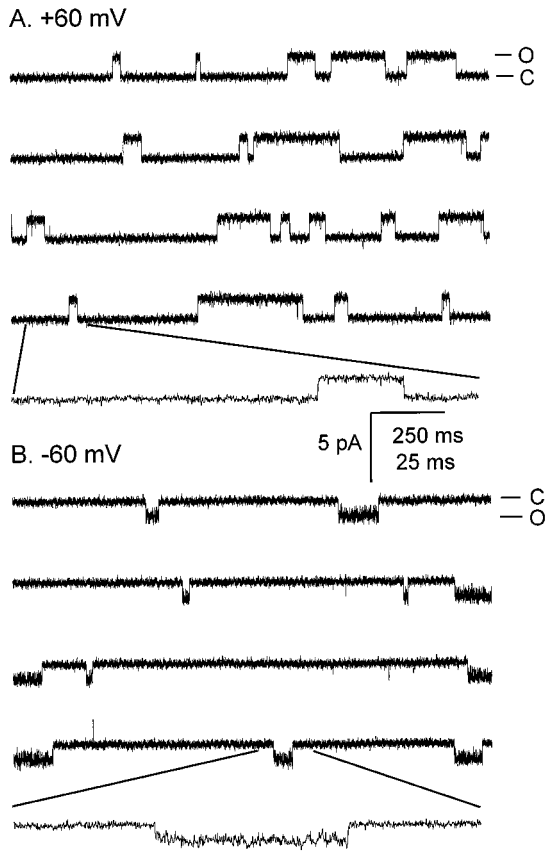

Fig. 2. Consecutive current traces from a single channel in response to 50 μM cAMP. A, +60 mV; B. −60 mV. One section in A and one in B are redisplayed on a 10× expanded time scale. C and O indicate open and closed current level. Note increased open-channel noise at −60 mV.

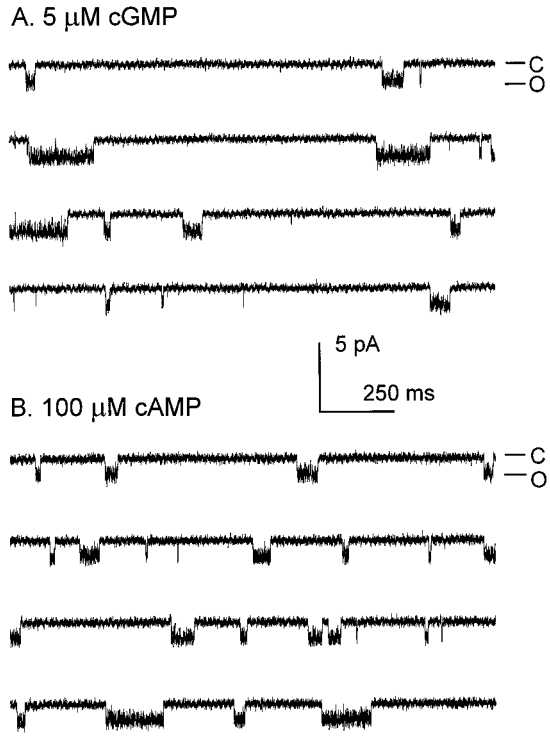

Fig. 3. Consecutive current traces of a channel recorded at −60 mV. A, 5 μM cGMP; B, 100 μM cAMP. C and O indicate open and closed current level. Note basic similarities in records.

ment the P_{open} was defined as the total open time divided by the total window length. These P_{open} values therefore do not necessarily represent the comparison between equal numbers of open intervals and closed intervals.

As expected, with increasing cAMP or cGMP, the open probability increased. Figure 5 shows the open- and closed-time histograms for a channel recorded at three different cAMP concentrations. The smooth lines are the sum of exponential functions that provided the best fits. The time constant and fractional area for the major component in each histogram are included in Table 1. It is apparent that the increase in open probability is associated both with greater open times (ranging from 32 ms at 50 μM to 194 ms at 250 μM) and with briefer closed times (ranging from 454 ms at 50 μM to 47 ms at 240 μM). This indicates that with more ligand molecules bound the open state is further stabilized, whereas the closed state is further destabilized.

Most of the recordings reveal one to two components in the open-time histograms or in the closed-time histograms. The lack of a long component (>1 s) in the closed-time histograms reflects the observation that rOCNC1 does not show clearly defined bursting behavior. Bursting is a feature of many well-studied ligand-gated channels, such as nicotinic acetylcholine receptors. The small number of components in dwell-time distributions, together with the absence of bursting, place constraints on the likely activation mechanisms (see below).

Fluctuations in P_{open}. Even in the presence of a constant concentration of agonist, the P_{open}s often showed strong fluctuations. Figure 6A plots the P_{open} of a channel during continuous activation by 5 μM cGMP. The 158-s period can be roughly divided into three segments, between which there are marked differences in channel activity. The division between segments I and II was supported by the observation that in the first ~20-s period the major closed intervals were longer than for the rest of the record and there was a discernible lack of brief closed intervals. The channel displayed relatively stable kinetics in segment II; and this portion of the data was selected for kinetic analysis. Figure 6B describes another channel, activated by 250 μM cAMP. The four recording periods in Fig. 6B were interrupted during the actual experiment by other operations, including switches to a different concentration or to another agonist. The channel entered segments II and IV with activity patterns different from the ones at the end of the previous segment. Also, the channel underwent spontaneous mode changes within segments II and IV, in a fashion similar to that shown in Fig. 6A. Segments I and III were relatively stable and comparable in P_{open}; they were regarded as representing a single channel "mode", and joined as one continuous record in further kinetic analysis.

None of the environmental conditions was changed during these fluctuations. These included the temperature of the room and the height of bath solution. It is therefore likely that the fluctuations reflect mode switches intrinsic to the channel. The switches develop during as little as three to six open and closing transitions.

A number of factors are known to modulate the activity of CNG channels. Phosphorylation (Gordon et al., 1992, 1995; Molokanova et al., 1997; Walters et al., 1998), calmodulin binding (Hsu and Molday, 1993; Chen and Yau, 1994; Liu et al., 1994; Molday, 1996), and thiol-modifying reactions may all play some role (Serre et al., 1995; Broillet and Firestein, 1996). In our recordings, the channels usually fluctuated

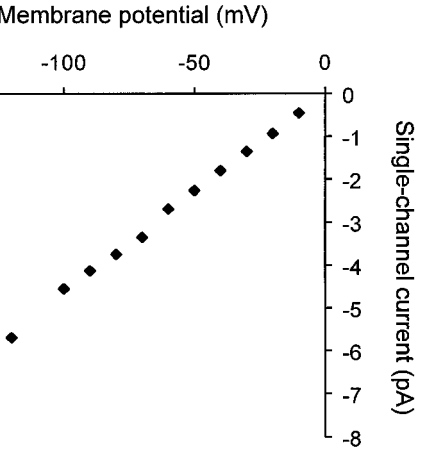

Fig. 4. An I-V plot of single-channel currents. Current levels recorded at a series of membrane potentials, from −10 mV to −150 V, are plotted against potentials.

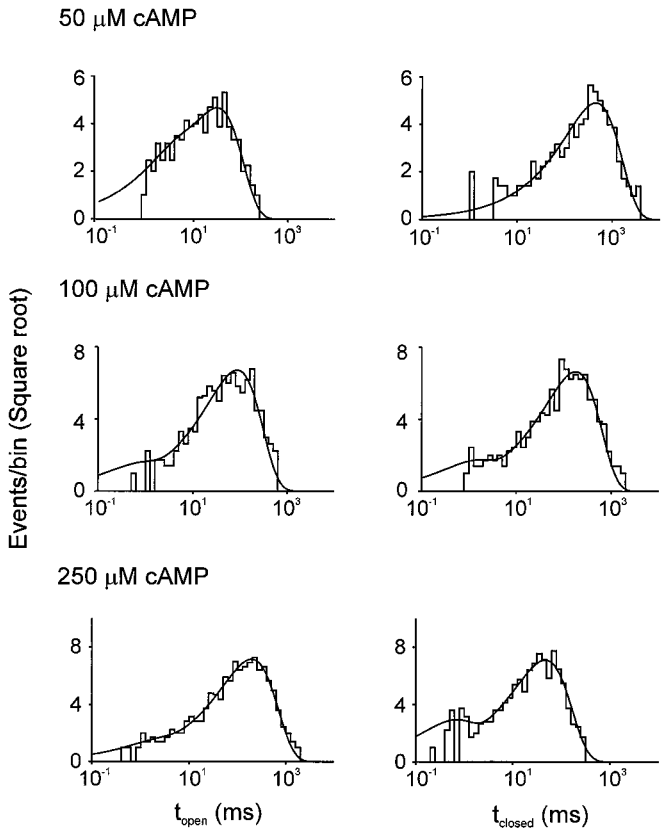

Fig. 5. Open- (left) and closed-time (right) histograms at three different cAMP concentrations. Smooth curves are sum of exponential functions used to fit observed distributions. Time constant and fractional area of major component in each histogram are given in Table 1.

TABLE 1
Parameters for channel analyzed in Fig. 4

cAMP	P_{open}	Major Open τ Area	Major Shut τ Area
μM	*%*	*ms*	*ms*
50	6.1	32 (84%)	454 (100%)
100	33	85 (97%)	175 (95%)
250	82	194 (98%)	47 (88%)

toward higher open probabilities, in other words, they became "sensitized". The sensitized channels required several minutes of washing with an agonist-free bath solution to revert to the initial sensitivities. In 10 to 20% of the patches, however, the recovery took place spontaneously, i.e., in the presence of the agonist. These observations indicate that the fluctuation cannot be directly explained by the usual irreversible processes, such as the gradual dilution of an intracellular modulatory protein following patch excision.

The fluctuations vitiate the accurate construction of dose-response plots from single-channel data by confounding the concentration-dependence of activities. We believe that the highly reproducible macroscopic dose-response relation is the result of averaging over independent fluctuations at many individual channels. Our subsequent kinetic analyses were necessarily restricted to time segments comprising, by visual inspection, relatively constant P_{open} values and open and closed times. Likewise, in our later comparison between cAMP and cGMP, the comparison was made between neighboring time segments, covering recordings during the last stable section of the first ligand and the beginning stable section of the second ligand. Furthermore, we usually compared segments that had similar P_{open} values.

Open-Channel Noise. As noted above, most of our analyses were performed at −60 mV to maintain stable seals and to avoid stretch-activated channels. At this membrane potential, the open channels display noticeable excess noise (Figs. 2B and 3). Previous studies suggest that noise during CNG channel openings arises primarily from open-channel block by Ca^{2+} or protons (Root and MacKinnon, 1994). Therefore the open-channel noise would not be expected to depend on the agonist; but we sought to test this point directly.

We analyzed the open-channel noise for cAMP and cGMP by filtering at 10 kHz and digitizing at 50 kHz. Power spectra were calculated using fast Fourier transformation, and the difference between the powers in the presence and the absence of cyclic nucleotides were fitted to the sum of a Lorentzian term plus a constant term and are shown in Fig. 7. For either cAMP or cGMP, a single Lorentzian component was adequate for describing the power spectrum. The power level and the characteristic frequency of the Lorentzian function were very similar between the two agonists. The constant component presumably arises from one or more processes, such as shot noise, rapid conductance fluctuations, or unresolved gaps, whose major frequencies lie beyond the accessible frequency range (Sigworth, 1985). We conclude that

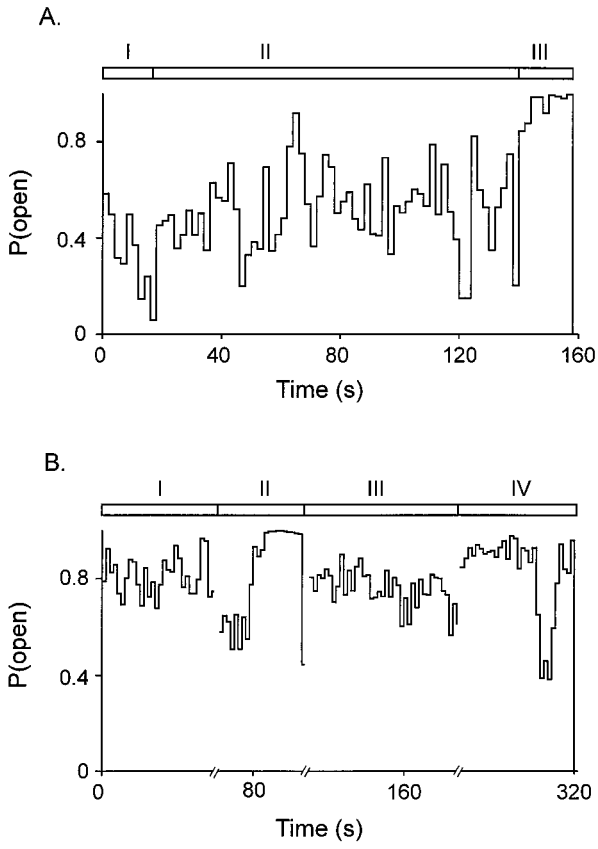

Fig. 6. Fluctuations of P_{open}. A and B, P_{open} for two different channels activated by 5 cGMP and 250 cAMP, respectively. Three segments in A are contiguous recording periods demonstrating direct switching between different "modes" of activation, whereas four segments in B are unconnected recording periods, between which the channel was exposed to other cAMP concentrations or to a different agonist. P_{open} values were calculated within 2-s time windows.

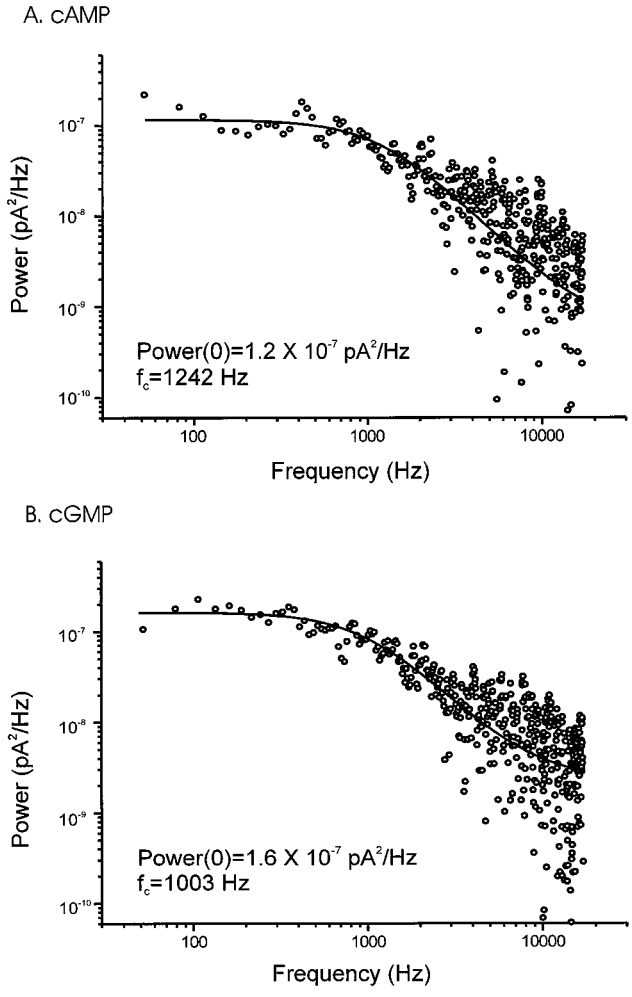

Fig. 7. Two cyclic nucleotides produce indistinguishable open-channel fluctuations. Power spectra of single channel current activated by 250 μM cAMP (A) and 5 μM cGMP (B). Data were calculated by subtracting spectra in the absence of cyclic nucleotides from spectra in the presence of cyclic nucleotides. Smooth lines represent fits to single Lorentzian functions. Corner frequencies and zero frequency power levels are indicated. Frequency-independent power offsets were, for A and B respectively, 5.7×10^{-10} pA^2/Hz and 2.3×10^{-9} pA^2/Hz.

within the frequency range of the recordings, the fluctuations of open-channel current induced by the two agonists have similar kinetics. There is therefore no indication that one agonist differs from the other by fluctuating among additional, short-lived states.

Kinetic Properties: Comparisons between Agonists. Figures 8 and 9 present our kinetic analyses in three separate recordings, each on a single channel that was tested with both cGMP and cAMP. Although the details of the most likely model vary among experiments, certain unifying characteristics appear.

The upper panel of Fig. 8A plots P_{open} against elapsed time for a channel activated by 5 μM cGMP during a 68-s period. The overall P_{open} for the entire period was 26.9%. The corresponding panel in Fig. 8B plots the same channel activated by 250 μM cAMP during a 328-s period; in this case, the overall P_{open} was 20.6%. The middle and lower panels are the closed- and open-time histograms, respectively. The smooth lines are the fitted exponential functions. For both cAMP and cGMP the open times are fitted by one exponential component, with time constants of 27.2 ms for cAMP and 33 ms for cGMP. The closed times were also similar between the two agonists; both can be described by the sum of two exponential functions: 0.47 ms (5%) and 106 ms (95%) for cAMP, and 0.35 ms (10%) and 89 ms (90%) for cGMP.

The simple kinetic model that has two closed states and one open state (Fig. 8, C and D, upper panel) is adequate to account for such dwell-time distribution patterns. Each horizontal arrow represents the binding (toward left) or dissociation (toward right) of a single agonist molecule, whereas each vertical arrow represents the opening (downward) or the closing (upward) of the channel. The parameters are rate-constant estimates obtained from the maximum-likelihood method. The units are $\mu M^{-1}\ s^{-1}$ or s^{-1} where appropriate. For cGMP, the series of 1080 events returned a log likelihood score of 2019, which can be improved to 2028 if we add one binding reaction preceding C1, with an association rate constant of 2.3 $\mu M^{-1}\ s^{-1}$ and dissociation rate constant of 3.9 s^{-1}. According to the likelihood ratio testing criterion (Horn, 1987), in a χ^2 distribution an increase of 9 in log likelihood score for two more parameters represents a 0.01 significance level, which by itself could be regarded as moderately significant. Yet considering the kinetic pattern of other channels that we have observed (see subsequent sections), the simpler model shown in Fig. 8C could be justified. The smooth curves in the middle and lower panels of Fig. 8, C and D are theoretical probability density functions calculated from the parameters shown in the upper panels.

For cAMP, the series of 4925 events yielded a log likelihood score of 9465, and this cannot be significantly improved by any alternative models, including the one that adds an extra closed state to the left of C1. The parameters are within a factor of 2 of those of cGMP, with the exception of the forward binding rate. This parameter for cAMP is 40-fold less than for cGMP and therefore accounts for nearly the entire difference in the effective concentrations of the two cyclic nucleotides.

The distribution pattern shown in Fig. 8, with a single exponential component in the open times, and two in the closed times, represents only a subset of the recorded channels. Other dwell-time distribution patterns have also been

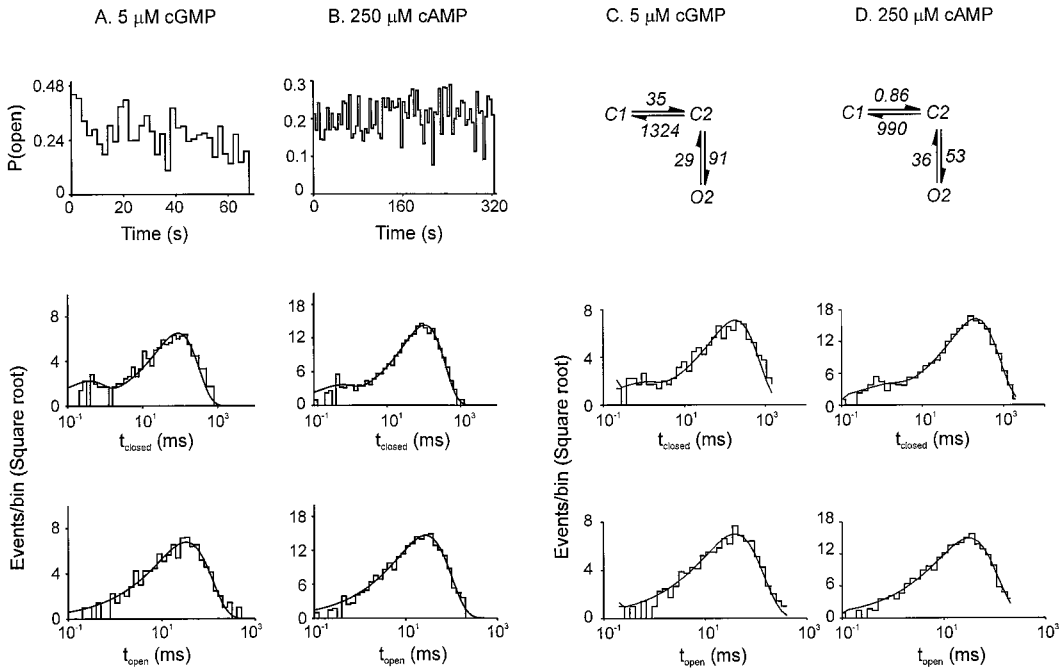

Fig. 8. A comparison between cAMP and cGMP. A and C, activation by 5 μM cGMP; B and D, activation by 250 μM cAMP. A and B, upper panels, P_{open} plots (data are plotted for successive 2- and 4-s intervals, respectively); middle and lower panels, closed- and open-time histogram, respectively, with fitting by sums of exponential functions. For both cAMP and cGMP, open times are fitted by a single component, shown by superimposed curves, whereas closed times require two components. C and D, upper panel, simplest kinetic models that can account for observations. Each horizontal arrow represents binding (toward left) or dissociation (toward right) of a single agonist molecule, whereas each vertical arrow represents opening (downward) or closing (upward) of channel. Middle and lower panels, same histograms as in A and B, with superimposed theoretical pdfs calculated from most likely kinetic parameters. These parameters are shown in kinetic models in lower panels. Units are $\mu M^{-1}\ s^{-1}$ or s^{-} where appropriate. Ratios of rate constants for each transition, i.e., equilibrium binding and gating constants, are documented in Table 2 together with the exponential fitting parameters and other information about data set.

observed; yet the similarity between cAMP and cGMP was often maintained. In the example of Fig. 9A, the recordings were fitted by two exponential components in both the open times and the closed times, both for activation by 5 μM cGMP and by 100 μM cAMP (these plots are omitted from Fig. 9 for simplicity). In fitting to kinetic models, as shown in Fig. 9A, we find it necessary to add another closed state, C0, to the left of C1. Again the major difference between cGMP and cAMP appears to lie in the binding steps; in this case cAMP binds ~190- and 3.5-fold more slowly in the first and second binding steps and dissociates ~230-fold more slowly from the first site.

Figure 9B shows analyses of a channel fitted best by kinetic models of differing structure for the two agonists. There were two closed-time components for both cAMP and cGMP, yet in open times, there were apparently two components for cGMP, but only one for cAMP.

Table 2 documents the key parameters for Figs. 8 and 9, A and B, such as the record duration, number of events, time constants, and fractional areas of the fitted exponential functions and the kinetic parameters derived from the maximum likelihood fitting.

Kinetic Properties: Concentration Dependence. We also performed simultaneous fits of data recorded at several different concentrations for a given channel. This was done by scaling the ligand association rate constants with the ligand concentrations for individual data sets, and optimizing the total likelihood of the combined data. We found that such global fittings generally provided less satisfactory results than fitting the data sets separately, i.e., without the constraint of holding the association rate constants in proportion to concentration. For instance, if a model that adequately fits two concentrations separately was used to fit the two data sets simultaneously, the predicted dwell-time probability density functions (pdfs) usually had noticeably poorer "goodness-of-fit" to the observed histograms than fitting separately.

In the example shown in Fig. 10, we fitted event series recorded at 100 μM cAMP (1361 events) and 250 μM cAMP (1401 events). Both records could be separately fit satisfactorily by the model comprising two closed states and one open state (such as the one in Fig. 8). When this model was fitted simultaneously to the two records, the log likelihood score, 4628, was much less than 4759, the sum of the separate scores (2092 and 2667 for 100 μM and 250 μM, respectively). Accompanying the deficient likelihood score is a poor fit to the interval duration histograms (not shown). However, if we allowed ligand binding to the open state O2 (O2-O3 transitions in Fig. 10C), the score improved by 78, to 4706. There were also improvements in the agreement between the observed and predicted histograms, particularly the open-time histograms. To further improve the fitting to the closed-time histograms, we added another binding event before C1 (C0-C1 transitions), and obtained a likelihood score of 4749, and satisfactory pdfs shown in Fig. 10, A and B. The model that comprises three closed states and two open states but forbids binding to open states (as shown in Fig. 9A) fitted less well (log likelihood score 4726), primarily because two uncon-

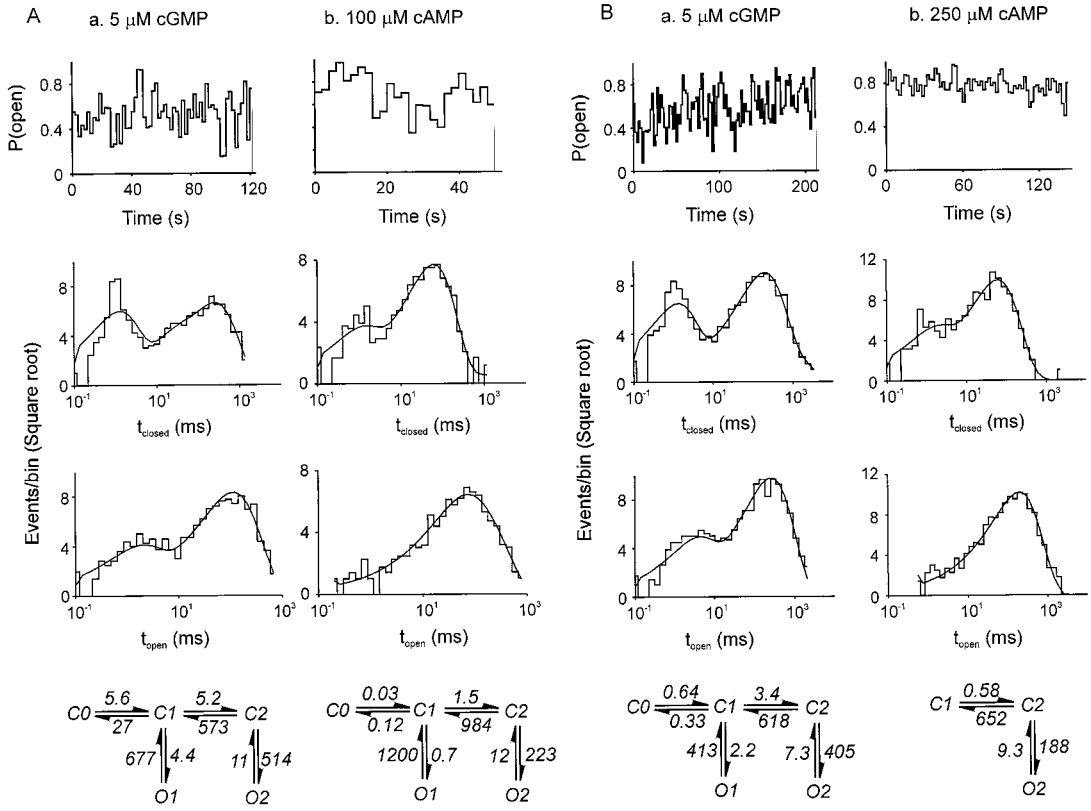

Fig. 9. Two other comparisons between cAMP and cGMP. A, a channel tested with activation by 5 μM cGMP (a) and with 100 μM cAMP (b). B, a channel tested with activation by 5 μM cGMP (a) and with 250 μM cAMP (b). Upper panels, P_{open} plots; middle and lower panels, closed- and open-time histograms, respectively. Lines represent theoretical pdfs calculated from most likely kinetic parameters. These parameters are shown in kinetic models in lower panels. Units are $\mu M^{-1} s^{-1}$ or s^{-1} where appropriate. Ratios of rate constants for each transition, i.e., equilibrium binding and gating constants, are documented in Table 2 together with exponential fitting parameters and other information about data set.

nected open states cannot account for the gradual changes of the time constant of open times. In fact, the gradual lengthening of open times at higher concentrations, rather than the shift in relative weights of fixed-length open time components (Fig. 5), implies that ligand binding not only connects closed states, but also open states. That ligand binding lengthens the open state provides a mechanism for the apparent cooperativity of the response to cyclic nucleotides. The fitted rate constant for the 02 ← 03 transition, ~20,000 s^{-1}, should be regarded as an estimate, because events of such duration are too brief for resolution by our recording system.

Discussion

Our experiments use modern single-channel kinetic analysis to deduce the mechanism of cyclic nucleotide channel activation. We studied homomultimeric channels formed by the rat olfactory cyclic nucleotide-gated channel α subunit. We observed that this channel has a single, full-conductance level even at very low cyclic nucleotide concentrations, allowing for detailed kinetic analysis. In other recent studies, other CNG channels have had several open conductance values (Ruiz and Karpen, 1997), and these variations have been used to deduce facts about stoichiometry and order of the subunits (Liu et al., 1996; Liu et al., 1998).

cAMP and cGMP Differ Primarily in Binding Affinities. One significant finding in this study is the similarity between cAMP and cGMP in the parameters that govern the open-closed transitions for liganded channels. This result was unexpected, because previous studies on macroscopic responses were interpreted to suggest that cGMP binds with similar affinity to cAMP, but then is more likely to open the channel (Varnum et al., 1995; Gordon and Zagotta, 1995a,b). Our conclusion of dissimilar binding but similar subsequent conformational changes is of course quite consistent with the findings that cAMP and cGMP induce equal maximal macroscopic conductances (Fig. 1; see also Gordon and Zagotta, 1995a). A greater gating equilibrium constant for cGMP (Ls in Table 2), would be associated either with more stabilized open states, or more destabilized closed states, or both. None of these differences was observed in our recordings: when the comparison was made at similar open probabilities, the open and closed times were comparable between cAMP and cGMP. Our experiments resolve events as fast as ~90 μs, and follow the channel activity for 10 to 20 min. Within this time frame, the lack of significant difference between cAMP and cGMP is true for most of the channels recorded, despite the differences in the detailed model that accounted for the data among recordings. The only noticeable exception is that some channels showed one more closed-time component with cGMP than with cAMP. Noise analysis on open channels would be expected to reveal—or at least to suggest—major differences in conductance substates or gating kinetics not clearly resolved by the single-channel recordings; but no such differences were found (Fig. 7), again arguing against differences other than at the binding steps.

We give a quantitative example of the difference between earlier conclusions and our own. The model adopted by Gordon and Zagotta (1995b) included independent binding at two equivalent sites and an opening transition from the doubly liganded state. In fitting the macroscopic dose-response relations, these authors found that the affinities for both cAMP and cGMP were approximately 286 μM, yet the allosteric gating constant L was 10^4 for cGMP and 8.9 for cAMP, a difference of more than 10^3-fold. In our study, however, for the channel shown in Fig. 8, the dissociation constants for cAMP and cGMP were estimated to be 1157 μM and 38 μM, respectively, a difference of over 30-fold. In contrast, the L values were 1.5 for cAMP and 3.1 for cGMP, different by slightly more than 2-fold. For the two channels shown in Fig. 9, A and B, cGMP has two to three times greater probability than cAMP for the second conformational change, yet the affinity at the second binding site is about six times higher. As the macroscopic EC_{50} of cGMP is about 30 times smaller than that of cAMP (Bradley et al., 1994; Fig. 1), a major portion of this difference is explained by differences in binding rather than gating.

In models that invoke two binding events (Fig. 9, A and B), where each bound state is able to open, we found that the first binding event has the weaker gating transition (smaller L), but the higher affinity. This lends support to the idea that each agonist molecule has to partition its finite capability for physical interactions into binding and gating. A similar trend in the usage of binding energy has been noted for the nicotinic acetylcholine receptors (Jackson, 1989).

Cooperativity Arises Partially Because Agonist Binds To Open State. A second significant finding in this

TABLE 2
Key parameters of channels analyzed in Figs. 8 and 9, A, and B

Agonist (μM)	Fig. 8		Fig. 9A		Fig. 9B	
	cGMP 5	cAMP 250	cGMP 5	cAMP 100	cGMP 5	cAMP 250
Duration (s)	68	328	122	52	216	146
No. events	1080	4925	1574	924	2071	2121
P_{open} (%) (mean ± S.D.)	26.9 ± 8.3	20.6 ± 6.6	51.5 ± 16.5	69.6 ± 15.7	56.8 ± 20.3	78 ± 8.7
τ_{c1} (A_{c1})	0.35 (10%)	0.47 (5%)	0.81 (50%)	0.58 (20%)	0.84 (39%)	0.59 (26%)
τ_{c2} (A_{c2})*	89 (90%)	106 (95%)	127 (50%)	39 (80%)	116 (61%)	33 (74%)
τ_{o1} (A_{o1})	33 (100%)	27 (100%)	1.7 (22%)	0.35 (4%)	2.4 (22%)	104 (100%)
τ_{o2} (A_{o2})*			103 (78%)	72 (96%)	143 (78%)	
Log of likelihood	2019	9465	3255	1833	3518	4061
L_1*			6.5×10^{-3}	5.5×10^{-4}	5.3×10^{-3}	
L_2	3.1	1.5	47	19	55	20
K_1 (μM)*			4.8	4	0.52	
K_2 (μM)	38	1157	110	656	182	1124

Abbreviations: τ, time constant of an exponential component in milliseconds; A, fractional area of an exponential component; c, closed times; o, open times; 1 and 2, first or second component; *, "where applicable", some channels lack a second component in histogram; K, equilibrium dissociation constant; L, equilibrium gating constant, equals opening rate constant divided by closing rate constant.

study is that cyclic nucleotide can bind to the open state, and that the open state is open longer with additional bound agonist molecules. This result could only be obtained with a kinetic approach like that used here. In the example of Fig. 10, the second binding would lengthen the open state by a factor of ~2 at a concentration of 55 μM cAMP. Because the EC_{50} for cAMP is 78 μM, this lengthening of the open state also contributes importantly to the sigmoid start of the dose-response relation.

In brief, we find that cooperativity arises from two separate mechanisms. 1) All our experiments reveal at least one binding step that opens the channel. In addition, some experiments (e.g., that shown in Fig. 9A) reveal a greater opening rate after the binding of a second bound cyclic nucleotide molecule. We do not consider it disturbing that only some of our experiments reveal this second binding, because our recordings also contain spontaneous fluctuations that presumably represent real changes in the underlying mechanism of opening. 2) Experiments with varying cyclic nucleotide concentrations also show that an additional agonist molecule can bind to the open state, prolonging the open state. These two mechanisms together produce the Hill coefficient between two and three usually measured for CNG-activated channels.

Our most complex model (that shown in Fig. 10) invokes the binding of three cyclic nucleotide molecules. It is formally possible that a fourth molecule binds as well, in a step either to the left or to the right of those explicitly identified in our study; this could further increase cooperativity. Together with other recent studies (Liu et al., 1996, 1998; Ruiz and Karpen, 1997), the present study represents progress toward a comprehensive kinetic description for these important and intriguing ion channels.

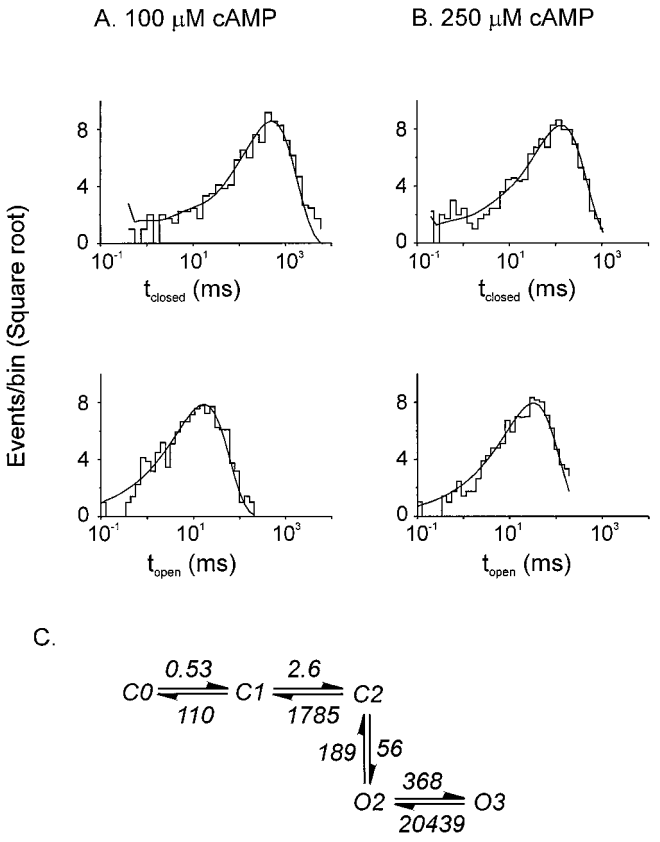

Fig. 10. Simultaneous fitting of data obtained at two cAMP concentrations. A, 100 μM; B, 250 μM. C, A model that provides an adequate fit to both records simultaneously. Theoretical pdfs calculated from kinetic parameters shown in C are superimposed as smooth lines in A and B.

Acknowledgments

We thank Yinong Zhang for much technical assistance and helpful discussions, Hairong Li and Brad Henkle for preparing oocytes, and Ben Edelman (Harvard College) for help using the MIL programs. We thank Dr. William Zagotta for insightful discussions during this project.

References

Bradley J, Li J, Davidson N, Lester HA and Zinn K. (1994) Heteromeric olfactory cyclic nucleotide-gated channels: A subunit that confers increased sensitivity to cAMP. *Proc Natl Acad Sci USA* **91:**8890–8894.

Broillet M-C and Firestein S (1996) Direct activation of the olfactory cyclic nucleotide-gated channel through modification of sulfhydryl groups by NO compounds. *Neuron* **16:**377–385.

Bucossi G, Nizzari M and Torre V (1997) Single-channel properties of ionic channels gated by cyclic nucleotides. *Biophys J* **72:**1165–1181.

Chen T-Y and Yau K-W (1994) Direct modulation by Ca^{2+}-calmodulin of cyclic nucleotide-activated channel of rat olfactory receptor neurons. *Nature* **368:**545–548.

Colquhoun D and Sigworth FJ (1995) Practical analysis of records, in *Single Channel Recording* (Sakmann B and Neher E eds.) pp 483–585, Plenum Press, New York.

Dhallan RS, Yau K-W, Schrader KA and Reed RR (1990) Primary structure and functional expression of a cyclic nucleotide-activated channel from olfactory neurons. *Nature* **347:**184–187.

Fesenko EE, Kolesnikov SS and Lyubarsky AL (1985) Induction by cyclic GMP of cationic conductance in plasma membrane of retinal rod outer segment. *Nature* **313:**310–313.

Finn JT, Grunwald ME and Yau K-W (1996) Cyclic nucleotide-gated ion channels: An extended family with diverse functions. *Annu Rev Physio.* **58:**395–426.

Frings S, Lynch JW and Lindemann B (1992) Properties of cyclic nucleotide-gated channels mediating olfactory transduction Activation, selectivity, and blockage. *J Genl Physiol* **100:**45–67.

Gordon S and Zagotta W (1995a) A histidine residue associated with the gate of the cyclic nucleotide-activated channels in rod photoreceptors. *Neuron* **14:**177–183.

Gordon S and Zagotta W (1995b) Localization of regions affecting an allosteric transition in cyclic nucleotide-activated channels. *Neuron* **14:**857–864.

Gordon S, Brautigan D and Zimmerman A (1992) Protein phosphatases modulate the apparent agonist affinity of the light-regulated ion channel in retinal rods. *Neuron* **9:**739–748.

Gordon S, Downing-Park J, Tam B and Zimmerman A (1995) Diacylglycerol analogs inhibit the rod cGMP-gated channel by a phosphorylation-independent mechanism. *Biophys J* **69:**409–417.

Horn R (1987) Statistical methods for model discrimination: Applications to gating kinetics and permeation of the acetylcholine receptor channel. *Biophys J* **51:**255–263.

Hoshi T, Zagotta WN and Aldrich RW (1994) *Shaker* potassium channel gating I: Transitions near the open state. *J Gen Physiol* **103:**249–278.

Hsu Y-T and Molday RS (1993) Modulation of the cGMP-gated channel of rod photoreceptor cells by calmodulin. *Nature* **361:**76–79.

Ildefonse M, Crouzy S and Bennett N (1992) Gating of retinal rod cation channel by different nucleotides: Comparative study of unitary currents. *J Membr Biol* **130:**91–104.

Jackson MB (1989) Perfection of a synaptic receptor: Kinetics and energetics of the acetylcholine receptor. *Proc Natl Acad Sci USA* **86:**2199–2203.

Li J and Lester H (1999) Functional roles of aromatic residues in the ligand-binding domain of cyclic nucleotide-gated channels. *Mol Pharmacol* **55:**873–882.

Li J, Zagotta WN and Lester HA (1997) Cyclic nucleotide-gated channels: Structural basis of ligand efficacy and allosteric modulation. *Q Rev Biophys* **30:**177–193.

Liman ER and Buck LB (1994) A second subunit of the olfactory cyclic nucleotide-gated channel confers high sensitivity to cAMP. *Neuron* **13:**611–621.

Liman ER, Tytgat J and Hess P (1992) Subunit stoichiometry of a mammalian K^+ channel determined by construction of multimeric cDNAs. *Neuron* **9:**861–871.

Liu M, Chen T-Y, Ahamed B, Li J and Yau K-W (1994) Calcium-calmodulin modulation of the olfactory cyclic nucleotide-gated cation channel. *Science* **266:**1348–1354.

Liu DT, Tibbs GR, Paoletti P and Siegelbaum SA (1998) Constraining ligand-binding site stoichiometry suggests that a cyclic nucleotide-gated channel is composed of two functional dimers. *Neuron* **21:**235–248.

Liu DT, Tibbs GR and Siegelbaum SA (1996) Subunit stoichiometry of cyclic nucleotide-gated channels and effects of subunit order on channel function. *Neuron* **16:**983–990.

Matthews G and Watanabe S-I (1988) Activation of single channels from toad retinal rod inner segments by cyclic GMP: Concentration dependence. *J Physiol (Lond)* **403:**389–405.

Molday RS (1996) Calmodulin regulation of cyclic-nucleotide-gated channels. *Curr Opin Neurobiol* **6:**445–452.
Molokanova E, Trivedi B, Savchenko A and Kramer RH (1997) Modulation of rod photoreceptor cyclic nucleotide-gated channels by tyrosine phosphorylation. *J Neurosci* **17:**9068–9076.
Nakamura T and Gold GH (1987) A cyclic nucleotide-gated conductance in olfactory receptor cilia. *Nature* **325:**442–444.
Qin F, Auerbach A and Sachs F (1996) Estimating single channel kinetic parameters from idealized patch-clamp data containing missed events. *Biophys J* **70:**264–280.
Qin F, Auerbach A and Sachs F (1997) Maximum Likelihood estimation of aggregated Markov process. *Proc R Soc Lond Biol Sci* **264:**375–383.
Quick MW and Lester HA. (1994) Methods for expression of excitability proteins in *Xenopus* oocytes, in *Ion Channels of Excitable Cells* (Narahashi T ed) pp 261–279, Academic Press, San Diego, CA.
Quick MW, Naeve J, Davidson N and Lester HA (1992) Incubation with horse serum increases viability and decreases background GABA transport in *Xenopus* oocytes. *BioTechniq* **13:**358–362.
Root MJ and MacKinnon R (1994) Two identical noninteracting sites in an ion channel revealed by proton transfer. *Science* **265:**1852–1856.
Ruiz M and Karpen JW (1997) Single cyclic nucleotide-gated channels locked in different ligand-bound states. *Nature* **389:**389–391.
Serre V, Ildefonse M and Bennett N (1995) Effects of cysteine modification on the activity of the cGMP-gated channel from retinal rods. *J Membr Biol* **146:**145–162.
Sesti F, Straforini M, Lamb TD and Torre V (1994) Gating, selectivity and blockage of single channels activated by cyclic GMP in retinal rods of the tiger salamander. *J Physiol (Lond)* **474:**203–222.
Sigworth FJ (1985) Open channel noise. I. Noise in acetylcholine receptor currents suggests conformational fluctuations. *Biophys J* **47:**709–720.
Sigworth FJ and Sine SM (1987) Data transformations for improved display and fitting of single-channel dwell time histograms. *Biophys J* **52:**1047–1054.
Stefani E, Toro L, Perozo E and Bezanilla F (1994) Gating of *Shaker* K^+ channels: I. Ionic and gating currents. *Biophys J* **66:**996–1010.
Taylor WR and Baylor DA (1995) Conductance and kinetics of single cGMP-activated channels in salamander rod outer segments. *J Physiol (Lond)* **483:**567–582.
Varnum M, Black K and Zagotta W (1995) Molecular mechanism for ligand discrimination of cyclic nucleotide-gated channels. *Neuron* **15:**619–625.
Walters RJ, Kramer RH and Nawy S (1998) Regulation of cGMP-dependent current in On bipolar cells by calcium/calmodulin-dependent kinase. *Vis Neurosci* **15:**257–261.
Yau K-W (1994) Cyclic nucleotide-gated channels: an expanding new family of ion channels. *Proc Natl Acad Sci USA* **91:**3481–3483.
Zimmerman AL and Baylor DA (1986) Cyclic GMP-sensitive conductance of retinal rods consists of aqueous pores. *Nature* **321:**70–72.
Zufall F, Firestein S and Shepherd GM (1994) Cyclic nucleotide-gated ion channels and sensory transduction in olfactory receptor neurons. *Annu Rev Biophys Biomol Struct* **23:**577–607.

Send reprint requests to: Dr. Henry A. Lester, Division of Biology 156-29, California Institute of Technology, Pasadena, CA 91125. E-mail: lester@caltech.edu